Regenerative Treatment of Peri-Implantitis Following Implant Surface Decontamination With Titanium Brush and Antimicrobial Photodynamic Therapy: A Case Series With Reentry

Pier Paolo Poli, DDS, MSc, PhD[1]
Francisley Ávila Souza, DDS, MSc, PhD[2]
Mattia Manfredini, DDS[1]
Carlo Maiorana, MD, DDS, MSc[1]
Mario Beretta, DDS, MSc, PhD[1]

Introduction

Peri-implantitis is a biofilm-induced inflammatory condition that affects both hard and soft tissues around osseointegrated dental implants.[1] Soft-tissue inflammation is clinically recognized by peri-implant bleeding on probing (pBOP) associated with increased peri-implant pocket probing depth (pPD), while progressive bone loss is identified on radiographs.[2] Unfortunately, emerging evidence suggests that pBOP and pPD may be considered as poor indicators of ongoing peri-implant pathology with a considerable false-positive rate together with a risk of iatrogenic damage by probing of dental implants.[3,4] Therefore, data gathered from pBOP and pPD should be associated with the radiographic assessment of crestal bone levels to obtain an incontrovertible diagnosis. It has been claimed, however, that intraoral radiography lacks the accuracy for assessing interproximal bone defect morphology[5] and often underestimates the intrasurgical bone loss at the correspondent site,[6] since the intraoperatively measured peri-implant bone levels tend to be more apical than the radiographic bone levels.[7] The suspected unreliability of intraoral radiographs in detecting the actual bone defect anatomy in the diagnostic phase can be transferred to the evaluation of peri-implant bone defect regeneration. Indeed, even more sophisticated radiologic examinations such as cone-beam computerized tomography, under certain conditions, may be inaccurate in assessing bone regeneration around augmented defects.[8] This is mainly due to metal artifacts masking osseointegration, shallow bony defects, and other peri-implant radiolucencies that may impede a correct evaluation of the residual bone architecture.[9]

All of these findings taken together seem to indicate that reentry surgery rather than pPD and radiographs may allow clinicians to precisely evaluate the actual 3-dimensional bone gain obtained following regenerative treatment of peri-implantitis defects. Interestingly, despite the questionable predictive value of clinical and radiologic examinations in the assessment of the residual bone defect after regenerative procedures, only few in vivo studies[10–18] have shown irrefutable images of the augmented bone at the reentry phase in humans. When it comes to peri-implantitis treatment, the goal is to remove all debris attached to the implant surface triggering the chronic inflammatory process.[2] These include biofilm alone, calculus, necrotic bone, or a combination of all of these elements. Several instruments have been proposed to decontaminate implant surfaces, including titanium brushes and antimicrobial photodynamic therapy (aPDT), with no clear evidence to support the superiority of a specific method over another.[19] Emerging evidence suggests that most chemical and mechanical protocols alone are not effective in completely removing the biological debris, so that only a partial decontamination can be achieved.[20] Therefore, it may be speculated that an efficacious response to peri-implantitis treatment is one that combines chemical and mechanical therapies.

In view of the above, the aim of the present study was to report the reentry phase after regenerative surgical therapy of peri-implantitis following combined mechanical and laser-assisted decontamination to allow direct visualization of the actual bone gain and the residual bone defect at each treated implant.

Materials and Methods

Study design

The present prospective investigation included patients diagnosed with peri-implantitis treated with a regenerative

[1] Implant Center for Edentulism and Jawbone Atrophies, Maxillofacial Surgery and Odontostomatology Unit, Fondazione IRCCS Cà Granda, Ospedale Maggiore Policlinico, University of Milan, Milan, Italy.
[2] Department of Surgery and Integrated Clinic, Araçatuba Dental School, São Paulo State University "Júlio de Mesquita Filho"–UNESP, Araçatuba–SP, Brazil.
* *Corresponding author,* e-mail: pierpaolo_poli@fastwebnet.it
https://doi.org/10.1563/aaid-joi-D-20-00093

approach. The diagnosis was established based on clinical and radiologic findings currently adopted in the diagnostic algorithm for peri-implant disease, namely, pBOP, pPD $\geq$6 mm, and radiographic evidence of bone loss $\geq$3 mm.[1] Furthermore, patients were enrolled if presenting with (1) no implant mobility, (2) presence of $\geq$2 mm of keratinized tissue, (3) treated chronic periodontitis and proper periodontal maintenance care, (4) no uncontrolled systemic diseases that may constitute contraindications to oral surgery procedures, (5) no concomitant therapies with antiresorptive agents including bisphosphonates and human monoclonal antibodies, and (6) nonsmoking or light smoking habits ($<$10 cigarettes per day). Patients were excluded if presenting clear indications of implant removal, such as nonretentive peri-implant bone defects associated with pPD $>$8 mm and a radiographic bone loss $>$50% of the implant length.[21] Patients unwilling to undergo further surgical interventions, thus preferring removable prosthetic solutions, were also excluded.

All patients were treated in a private practice setting on an outpatient basis under local anesthesia in accordance with the Declaration of Helsinki on ethical principles for medical research involving human subjects. All surgical procedures were performed by the same surgeon. Each subject was provided a detailed description of the treatment plan and was required to sign an informed consent form.

Surgical treatment

All patients were treated according to a standardized protocol involving mechanical and chemical decontamination of the implant surface and bone augmentation procedures.[18] In brief, paramarginal incisions were made to reflect mucoperiosteal flaps at the buccal and oral aspects. Granulation tissue was meticulously removed from the defect area, and the implant surface was debrided and instrumented using titanium curettes and rotary titanium brushes (Ti-Brush, Straumann, Basel, Switzerland) fixed on a surgical handpiece, oscillating in a clockwise/counterclockwise direction at low speed (800 rpm for 1 minute) under copious irrigation with sterile saline solution. Once the biofilm was macroscopically removed, aPDT was locally performed with a specific setup (HELBO, Bredent Medical, Senden, Germany). A solution of phenothiazine chloride dye consisting of methylenthioniniumchlorid (HELBO Blue Photosensitizer, Bredent Medical) was applied on the implant surface and surrounding tissues and left in place for 3 minutes. Subsequently, the surgical area was rinsed vigorously for 1 minute with sterile saline solution, and the photosensitizer was photo-activated at 6 sites per implant for 10 seconds each by means of a handheld 100-mW diode laser with a wavelength of 660 $\pm$ 10 nm (HELBO TheraLite Laser, Bredent Medical) equipped with a dedicated probe (HELBO 3D Pocket Probe, Bredent Medical) providing a power density of 60 mW/cm^2. Both the intrabony and the supracrestal components of the peri-implant defect were grafted with autogenous bone chips harvested from the neighboring area mixed with deproteinized bovine bone mineral (DBBM) particles (Bio-Oss, Geistlich, Wolhusen, Switzerland) in a 70:30 ratio. The graft was stabilized with a 0.2-mm-thick titanium mesh (KLS Martin, Tuttlingen, Germany) trimmed and adapted to the surgical defect to create a proper bone contour. A resorbable collagen membrane (Biogide, Geistlich) was finally applied over the titanium mesh. Periosteal horizontal releasing incisions were performed to mobilize the flaps and obtain a tension-free first-intention closure. The patient was instructed to rinse 3 times daily with 0.2% chlorhexidine mouthwash rinse solution for 1 minute starting 1 week prior surgery until 2 postoperative weeks. The antibiotic therapy consisted of 1 g amoxicillin clavulanate starting the day before the surgery twice daily for 6 days. Anti-inflammatory and analgesic therapy was prescribed (ibuprofen 600 mg, 3 times daily) during the first 2 days and according to the patients' individual needs thereafter.

After a submerged healing period ranging from 6 to 9 months, the reentry surgery was performed to remove the titanium mesh and reconnect the abutment and the prosthesis.

Clinical evaluations

In all sites, the clinical evaluations were performed by the second operator, who was blinded with respect to the study outcome. During the initial regenerative procedure (T_0) after flap elevation, each peri-implantitis lesion was classified according to the bone defect configuration as proposed by Schwarz and coworkers.[22] The overall vertical defect (oVD), defined as the distance from the top of the implant platform to the bottom of the bone defect, was measured at the level of the deepest aspect. The oVD was further divided into a supracrestal (sVD) and an intrabony (iVD) component. The sVD was measured as the linear distance from the alveolar bone crest to the implant platform, while the iVD was measured as the distance from the alveolar bone crest to the bottom of the defect. The measurements were performed with a periodontal probe (PCP-UNC 15, Hu-Friedy, Chicago, Ill) and rounded at the nearest half millimeter. The same measurements were registered at the reentry surgery (T_1) to calculate the overall vertical bone gain (oVBG) divided into a supracrestal (sVBG) and an intrabony (iVBG) bone augmentation with related percentages of defect resolution (DR) and residual defect classification. Data at the implant level were reported as mean values $\pm$ standard deviations using a commercially available statistical software (IBM SPSS Statistics 24.0, IBM Corp, Armonk, NY).

Results

A total of 6 adult patients (4 women, 2 men; mean age: 60.83 $\pm$ 4.09 years) diagnosed with peri-implantitis were included. Overall, 11 osseointegrated dental implants supporting single crowns or bridgework restorations were consecutively treated. The baseline demographic data and defect characteristics are presented in Table 1. For each case, the initial defect at T_0 and residual defect at T_1 are illustrated in Figures 1 through 6. Healing proceeded uneventfully in all patients. At the reentry surgery, no evidence of granulation tissue, purulence, or progressive bone resorption was found. Newly formed bonelike tissue hardly distinguishable from the existing bone was found in intimate contact with the implant surface at most of the implant sites. A modest amount of augmented bone was obtained at only 1 mandibular site, resulting in persistent dehiscence-type defects associated with a supracrestal component. The most frequently observed configurations of bone

Table 1

Implant characteristics and defects morphology at baseline*

Case No.	Age	Gender	Race	ASA	Implant Position	Implant Surface Topography	Diameter, mm	Length, mm	Defect Morphology†
1	61	F	Caucasian	II	30	Grit blasted and acid etched	5	11	II
					31	Grit blasted and acid etched	5	11	Ie + II
2	67	M	Caucasian	II	18	Grit blasted and acid etched	4	11	Ib + II
					19	Grit blasted and acid etched	5	11	Ie + II
3	65	M	Caucasian	II	8	Sand blasted and high temperature etched	3.5	12	Id
4	59	F	Caucasian	II	2	Zirconium sand blasted acid etched	4.25	11.5	II
					3	Zirconium sand blasted acid etched	4.25	11.5	Ic + II
5	55	F	Caucasian	II	2	Grit blasted and acid etched	4	11	Ic + II
					3	Grit blasted and acid etched	4	11	Ie
					4	Grit blasted and acid etched	4	11	Ic + II
6	58	F	Caucasian	II	12	Zirconium sand blasted acid etched	3.8	11.5	Id

*ASA indicates American Society of Anesthesiologists Physical Status Classification System; Class I, intrabony component; Class Ia, dehiscence-type component on the buccal aspect of the alveolar crest; Class Ib, buccal dehiscence with a semicircular component to the middle of the implant body; Class Ic, buccal dehiscence with a circumferential component under maintenance of the oral compacta; Class Id, circumferential defect in mesial and distal areas with dehiscence-type component on the buccal and oral aspect of the alveolar crest; Class Ie, circumferential defect with maintenance of the buccal and oral contours of the supporting crestal bone; Class II, supracrestal component.

†Defect morphology according to Schwarz et al.[16]

defects were Class Ic and Class Ie. Most bone defects were associated with a supracrestal component. The measurements recorded at T_1 are reported in Table 2. The mean oVD decreased from 4.22 $\pm$ 1.05 mm at T_0 to 1.13 $\pm$ 1.38 at T_1. This resulted in a mean oVBG of 3.09 $\pm$ 1.16 mm, which corresponded to a calculated overall mean DR score of 76.02% $\pm$ 25.5%. The mean sVD decreased from 2.93 $\pm$ 1.4 at T_0 to 1.78 $\pm$ 1.35 at T_1. The resultant mean sVBG was 1.37 $\pm$ 0.99 mm, corresponding to a calculated overall mean DR score of 50.82% $\pm$ 32.69%. With respect to the mean iVD, a decrease from 2.55 $\pm$ 1.01 mm to 0 mm was observed from T_0 to T_1, resulting in a mean DR score of 100%. At the reentry surgery, in all except 3 implants, at least 1 bone wall was present in intimate contact with the implant and reaching the top of the implant platform. Conversely, in 2 mandibular sites, supracrestal defects of different magnitude were still observed.

Discussion

A combined mechanical and chemical decontamination of contaminated implant surfaces together with regenerative procedures and submerged healing yielded promising results in terms of clinical healing and new bone formation. This was confirmed at the reentry surgery, which allowed direct visualization and quantitative measurement of the bone gain around each implant. The visual assessment of the regenerated peri-implantitis defect is crucial, as conventional clinical indices together with radiological examinations may not be considered completely trustworthy in the evaluation of the regenerative treatment outcome.

The use of a titanium brush aimed to disrupt the bacterial biofilm on the implant surface. The treated surface examined after the mechanical decontamination appeared smooth and clean, with no macroscopic evidence of persistent biofilm, a feature already reported by An and coworkers.[11] It is worth noting that titanium brushes are capable of effectively instrumenting the thread and valley areas, which may be considered as the most difficult-to-access regions of a contaminated implant.[23] This may explain the positive outcome achieved in the present study, highlighting the increased benefits in the additional use of titanium brushes during regenerative treatment of peri-implantitis.[24] It must be noted, however, that the effectiveness of the mechanical treatment has been verified visually with magnifying devices. The undercuts of the threads and the adhesion of biofilm in the porosity of microstructured roughened surfaces may render the mechanical treatment still unpredictable. The adjunctive use of chemical decontamination methods should be contemplated to remove any residual biofilm remnants and destroy the organic components of bacteria still attached to the implant surface. In peri-implantitis lesions, a heterogeneous mixed infection can be detected, with a certain prevalence of *Aggregatibacter actinomycetemcomitans*, *Prevotella intermedia*, *Porphyromonas gingivalis*, and *Tannerella forsythia*.[25] It is noteworthy that both gram-positive and gram-negative bacteria have an overall negatively charged cell surface, which acts as an electroattractive scaffold for cationic photosensitizers.[26] Thus, the use of cationic phenothiazinium derivatives such as the phenothiazine chloride dye used in the present study may be extremely useful at peri-implantitis lesions because of their high binding affinity for both gram-positive and gram-negative bacteria. In this respect, the photosensitizer is able to access this multispecies biofilm at the most restricted regions of the implant microstructure, including the valley area and the micropores of rough surfaces. In addition, systemic toxicity is largely absent outside the irradiated zone, and no antimicrobial resistance is developed against the dye. All of these advantages taken together support the use of aPDT as an adjunctive treatment modality in case of peri-implant disease. The outcomes achieved in the present study fully agree with the results observed in a recent case series reporting improved crestal bone level changes following aPDT associated with regenerative therapy of peri-implantitis defects.[27] The authors reported a mean bone gain of 3.78 mm, which is similar to that

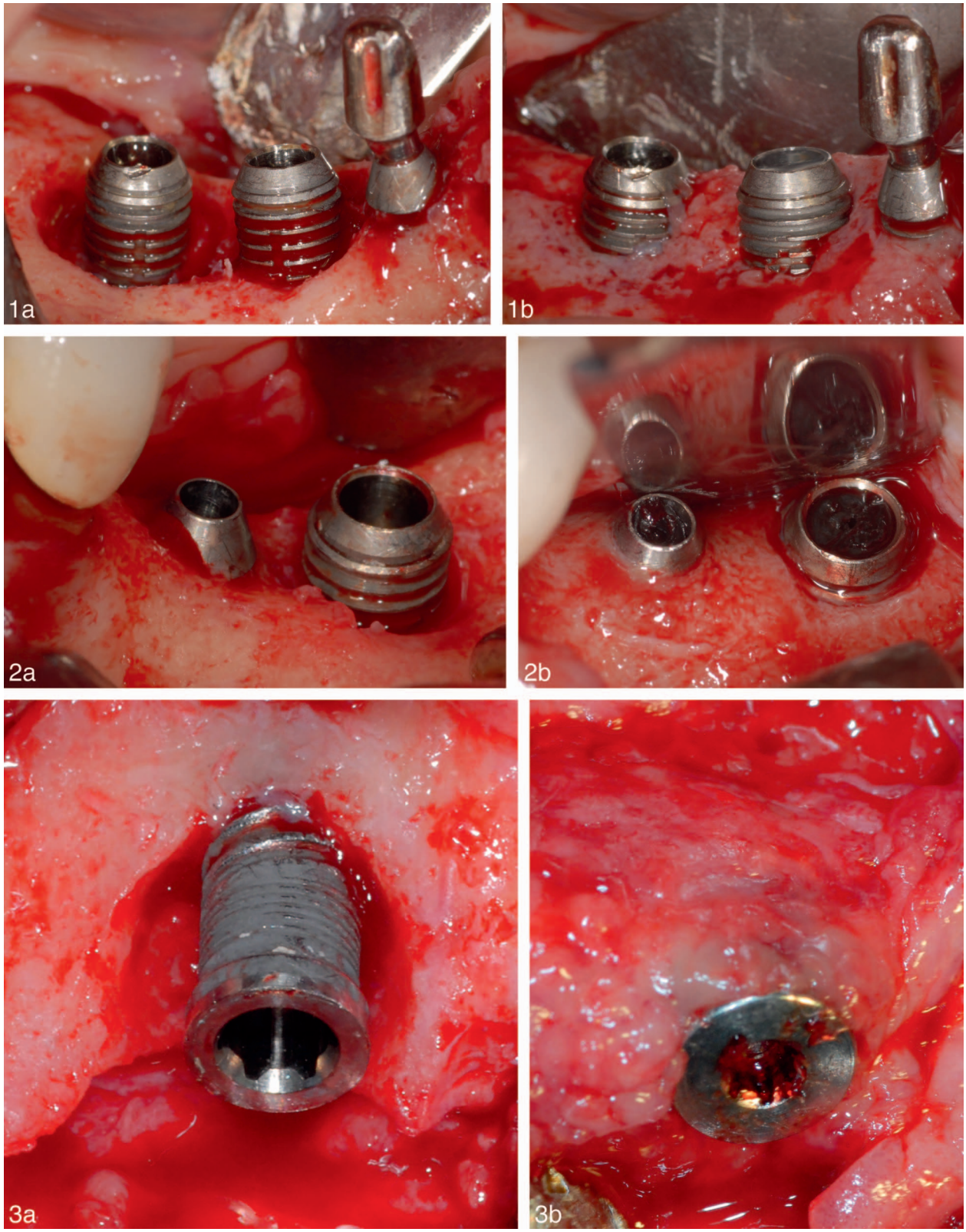

Figures 1–3. Figure 1. Clinical view of treatment progression in case 1. (a) Intrasurgical view of the peri-implant defects in positions 30 and 31 at T_0, (b) Intrasurgical view of the residual peri-implant defects at T_1. A supracrestal component is still visible associated with a dehiscence-type defect configuration. **Figure 2.** Clinical view of treatment progression in case 2. (a) Intrasurgical view of the peri-implant defects in positions 18 and 19 at T_0. (b) Intrasurgical view of the residual peri-implant defects at T_1. A supracrestal component of approximately 1 mm is visible around both implant necks associated with a dehiscence defect extended at the top of the first visible implant thread at the buccal aspect of implant 19. **Figure 3.** Clinical view of treatment progression in case 3. (a) Intrasurgical view of the peri-implant defect in position 8 at T_0. (b) Intrasurgical view of the regenerated peri-implant defect at T_1.

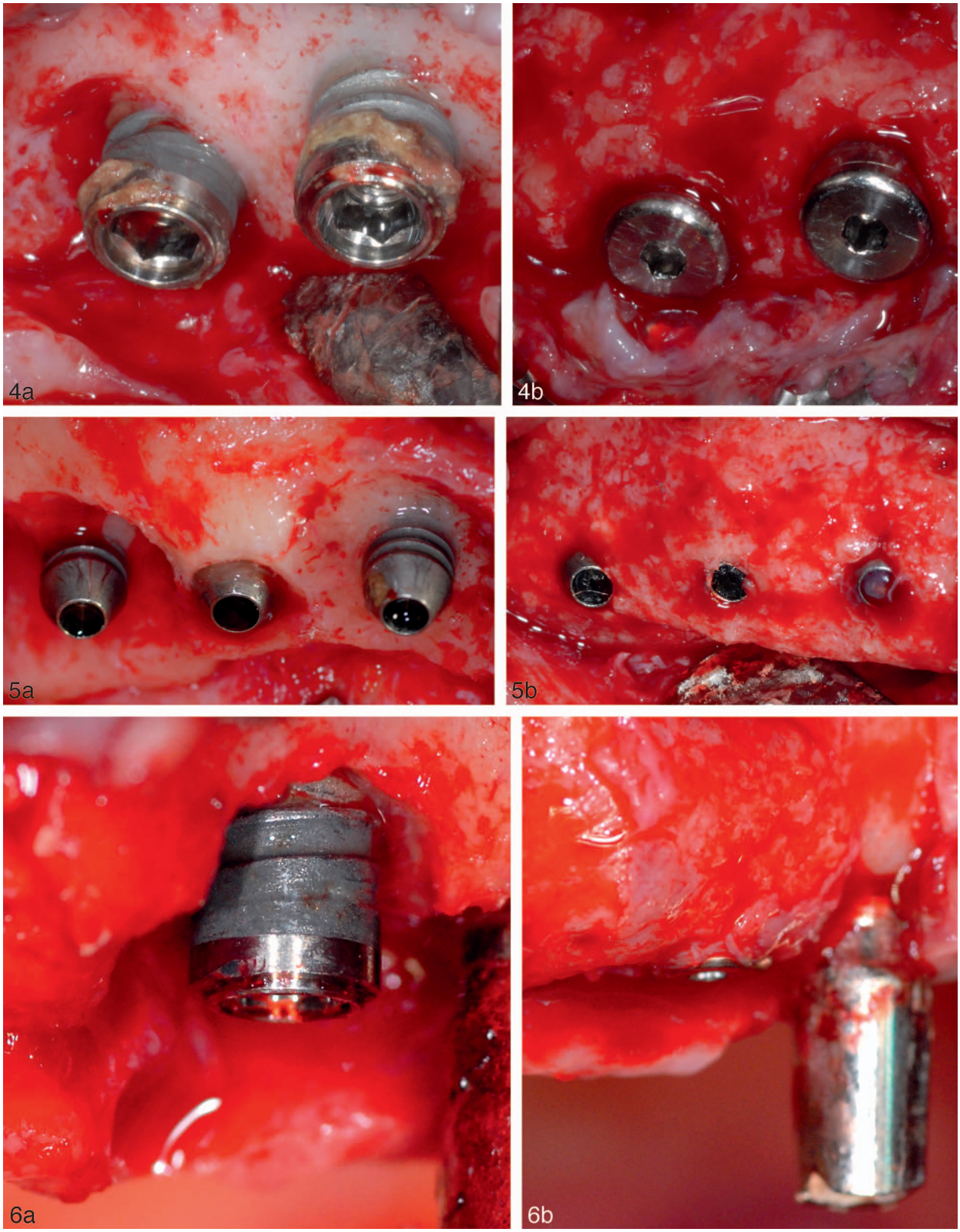

Figures 4–6. Figure 4. Clinical view of treatment progression in case 4. (a) Intrasurgical view of the peri-implant defects in positions 2 and 3 at T_0. (b) Intrasurgical view of the regenerated peri-implant defects at T_1. A dehiscence-type defect exposing the machined collar is visible at the buccal aspect of implant 3. **Figure 5.** Clinical view of treatment progression in case 5. (a) Intrasurgical view of the peri-implant defects in positions 2, 3, and 4 at T_0. (b) Intrasurgical view of the regenerated peri-implant defects at T_1. **Figure 6.** Clinical view of treatment progression in case 6. (a) Intrasurgical view of the peri-implant defect in position 12 at T_0. (b) Intrasurgical view of the regenerated peri-implant defect at T_1.

TABLE 2

Progression of clinical measurements from T_0 to T_1 and residual defect morphology observed at T_1*

	T_0			T_1						
Case No.	iVD, mm	sVD, mm	oVD, mm	iVBG, mm	iVBG, %	sVBG, mm	sVBG, %	oVBG, mm	oVBG, %	Residual defect morphology†
1	n/a	5	5	Absent	Absent	1.5	30	1.5	30	Ic
	2	4	6	2	100	0	0	2	33.3	II
2	1	2	3	1	100	1	50	2	66.6	II
	2	1.5	3.5	2	100	0.5	33.3	2.5	71.4	Ib + II
3	4	Absent	4	4	100	Absent	Absent	4	100	Complete resolution
4	Absent	5	5	Absent	Absent	3	60	3	60	Ia
	2.5	2.5	5	2.5	100	2.5	100	5	100	Complete resolution
5	2.5	2	4.5	2.5	100	2	100	4.5	100	Complete resolution
	2	Absent	2	2	100	Absent	Absent	2	100	Complete resolution
	2.5	1.5	4	2.5	100	0.5	33.3	3	75	Ia
6	4.5	Absent	4.5	4.5	100	Absent	Absent	4.5	100	Complete resolution

*VD indicates vertical defect; VBG, vertical bone gain; i, intrabony component; s, supracrestal component; o, overall defect component.
†Defect morphology according to Schwarz et al.[16]

obtained in the present study. Similarly, Schwarz and colleagues[16] found a mean defect augmentation of 3.5 mm corresponding to a calculated mean DR of 85% considering implants that healed uneventfully. The results reported herein favorably comply with those showed by Schlee and coworkers,[14] who measured mean bone gain values ranging from 2 to 4 mm depending on defect morphology. Higher values of mean bone gain have been observed at reentry following regenerative therapy of peri-implantitis. Froum and Rosen[13] found a mean bone fill of roughly 5 mm, ranging from 2 to 9 mm. However, it is worth mentioning that initial defect depths varied from 3 to 12 mm. In the present study, the fact that the oVD ranged from 2 to 6 mm may explain this discrepancy. Nevertheless, the mean percentage of bone fill was similar to that reported in the present study, namely, 73% and 76%, respectively. Accordingly, Parma-Benfenati and coworkers[15] reported a mean bone gain of almost 5 mm, with a mean pretreatment defect depth of approximately 5.5 mm at baseline, resulting in a mean bone fill of 91%. Interestingly, all implants that healed with a submerged approach and achieved complete defect fill had a machined surface. Conversely, the implants treated in the present study were characterized by rough surfaces. Thus, one may speculate that surface topography might play an important role in the prognosis of the treatment. In this regard, it should be noted that both titanium brushes and aPDT have a modest impact on implant surface modifications. A recent in vitro micro-topographical analysis showed that titanium brushes did not reveal significant changes in roughness parameters or surface chemical composition in sandblasted and acid-etched titanium disks as compared with untreated samples.[28] Similarly, Park and coworkers[29] did not observe any differences in surface roughness values after instrumenting sandblasted and acid-etched titanium disks with a commercially available titanium brush. At the same time, implants with sandblasted and acid-etched surfaces treated with aPDT did not show microscopical alterations such as melting, glossiness, cracking, ripple pattern, and slip-line formation following decontamination.[30] In the present study, at each site, the existing prosthesis was removed to perform tension-free flap release and ensure undisturbed healing. This crucial aspect has been confirmed by Wen and coworkers,[17] who stated that it is pivotal to achieve primary wound closure to ensure a successful and predictable outcome following regenerative therapy of peri-implantitis. The authors adopted a comparable approach to that reported in the present study, namely, debridement of inflamed granulomatous tissues, implant surface decontamination, grafting of the intrabony component with autogenous bone and DBBM, graft stabilization with nonresorbable membrane, and primary closure. An average bone gain of 96% was obtained, which is comparable with the mean bone fill of 100% achieved in the present study considering the intrabony defect component. This finding clearly points out that defects that are outside of the bony housing and defects beyond the line drawn between 2 adjacent bone contours may not be suitable for this approach. Indeed, in the present study, an overall mean DR score of 50% was observed for the supracrestal component, meaning that the regeneration of suprabony defects was not predictable. Thus, it might be suggested to manage supracrestal defects featured by consistent horizontal bone loss with implantoplasty procedures of exposed threads.[31] This could be particularly true in the posterior mandible, where supracrestal defects were not completely resolved in the present study. Apart from the reduced surgical access in the said region, unsatisfactory bone augmentation can be related to the native alveolar bone anatomy. The bone architecture is generally characterized by thick compact cortical bone and low blood supply with a consequent negative effect on bone regeneration in this region.[32] In addition, the flat morphology of the residual ridge did not allow proper containment of the bone graft along with the clot, further jeopardizing the regenerative outcomes. Because these factors apply to normal conditions, it is safe to assume that in compromised circumstances such as the regenerative treatment of infected implants, the posterior mandible is one of the most challenging anatomical sites to approach.

The data obtained in the present study might be useful for calculating an adequate sample size in future clinical trials aimed to evaluate the effectiveness of these methods used alone and combined. In this respect, it must be noted that the

results reported herein should be interpreted cautiously, because the single effect of each technique or a possible synergism cannot be extrapolated from the present case series.

Conclusion

Regenerative treatment of peri-implantitis following meticulous implant surface decontamination with titanium brush and aPDT showed promising results. The regenerative potential was strictly related to the defect morphology. Further confounding factors could not be identified because of the limited sample.

Abbreviations

aPDT: antimicrobial photodynamic therapy
DBBM: deproteinized bovine bone mineral
DR: defect resolution
iVBG: intrabony vertical bone gain
iVD: intrabony vertical defect component
oVBG: overall vertical bone gain
oVD: overall vertical defect
pBOP: peri-implant bleeding on probing
pPD: peri-implant pocket probing depth
sVBG: supracrestal vertical bone gain
sVD: supracrestal vertical defect component

Note

The authors whose names are listed in the present submission certify that they have no affiliations with or involvement in any organization or entity with any financial interest (such as honoraria; educational grants; participation in speakers' bureaus; membership, employment, consultancies, stock ownership, or other equity interest; and expert testimony or patent-licensing arrangements) or nonfinancial interest (such as personal or professional relationships, affiliations, knowledge, or beliefs) in the subject matter or materials discussed in this article. This clinical report did not receive any specific grant from funding agencies in the public, commercial, or not-for-profit sectors.

References

1. Renvert S, Persson GR, Pirih FQ, Camargo PM. Peri-implant health, peri-implant mucositis, and peri-implantitis: case definitions and diagnostic considerations. *J Clin Periodontol*. 2018;45(suppl 20):S278–S285.

2. Schwarz F, Derks J, Monje A, Wang HL. Peri-implantitis. *J Periodontol*. 2018;89(suppl 1):S267–S290.

3. Coli P, Sennerby L. Is peri-implant probing causing over-diagnosis and over-treatment of dental implants? *J Clin Med*. 2019;8:1123.

4. Hashim D, Cionca N, Combescure C, Mombelli A. The diagnosis of peri-implantitis: a systematic review on the predictive value of bleeding on probing. *Clin Oral Implants Res*. 2018;29(suppl 16):276–293.

5. Christiaens V, De Bruyn H, De Vree H, Lamoral S, Jacobs R, Cosyn J. A controlled study on the accuracy and precision of intraoral radiography in assessing interproximal bone defect morphology around teeth and implants. *Eur J Oral Implantol*. 2018;11:361–367.

6. Serino G, Sato H, Holmes P, Turri A. Intra-surgical vs. radiographic bone level assessments in measuring peri-implant bone loss. *Clin Oral Implants Res*. 2017;28:1396–1400.

7. Garcia-Garcia M, Mir-Mari J, Benic GI, Figueiredo R, Valmaseda-Castellon E. Accuracy of periapical radiography in assessing bone level in implants affected by peri-implantitis: a cross-sectional study. *J Clin Periodontol*. 2016;43:85–91.

8. Fienitz T, Schwarz F, Ritter L, Dreiseidler T, Becker J, Rothamel D. Accuracy of cone beam computed tomography in assessing peri-implant bone defect regeneration: a histologically controlled study in dogs. *Clin Oral Implants Res*. 2012;23:882–887.

9. Jacobs R, Vranckx M, Vanderstuyft T, Quirynen M, Salmon B. CBCT vs other imaging modalities to assess peri-implant bone and diagnose complications: a systematic review. *Eur J Oral Implantol*. 2018;11(suppl 1): 77–92.

10. Behneke A, Behneke N, d'Hoedt B. Treatment of peri-implantitis defects with autogenous bone grafts: six-month to 3-year results of a prospective study in 17 patients. *Int J Oral Maxillofac Implants*. 2000;15:125–138.

11. An YZ, Lee JH, Heo YK, Lee JS, Jung UW, Choi SH. Surgical treatment of severe peri-implantitis using a round titanium brush for implant surface decontamination: a case report with clinical reentry. *J Oral Implantol*. 2017;43:218–225.

12. Azzeh MM. Er, Cr:YSGG laser-assisted surgical treatment of peri-implantitis with 1-year reentry and 18-month follow-up. *J Periodontol*. 2008; 79:2000–2005.

13. Froum SJ, Rosen PS. Reentry evaluation following treatment of peri-implantitis with a regenerative approach. *Int J Periodontics Restorative Dent*. 2014;34:47–59.

14. Schlee M, Rathe F, Brodbeck U, Ratka C, Weigl P, Zipprich H. Treatment of peri-implantitis-electrolytic cleaning versus mechanical and electrolytic cleaning: a randomized controlled clinical trial-six-month results. *J Clin Med*. 2019;8:1909.

15. Parma-Benfenati S, Roncati M, Galletti P, Tinti C. Peri-implantitis treatment with a regenerative approach: clinical outcomes on reentry. *Int J Periodontics Restorative Dent*. 2015;35:625–636.

16. Schwarz F, John G, Becker J. Reentry after combined surgical resective and regenerative therapy of advanced peri-implantitis: a retrospective analysis of five cases. *Int J Periodontics Restorative Dent*. 2015;35: 647–653.

17. Wen SC, Huang WX, Wang HL. Regeneration of peri-implantitis infrabony defects: report on three cases. *Int J Periodontics Restorative Dent*. 2019;39:615–621.

18. Poli PP, Cicciu M, Beretta M, Maiorana C. Peri-implant mucositis and peri-implantitis: a current understanding of their diagnosis, clinical implications, and a report of treatment using a combined therapy approach. *J Oral Implantol*. 2017;43:45–50.

19. Khoury F, Keeve PL, Ramanauskaite A, et al. Surgical treatment of peri-implantitis—consensus report of working group 4. *Int Dent J*. 2019;(9 suppl 2):18–22.

20. El Chaar E, Almogahwi M, Abdalkader K, Alshehri A, Cruz S, Ricci J. Decontamination of the infected implant surface: a scanning electron microscope study. *Int J Periodontics Restorative Dent*. 2020;40:395–401.

21. Padial-Molina M, Suarez F, Rios HF, Galindo-Moreno P, Wang HL. Guidelines for the diagnosis and treatment of peri-implant diseases. *Int J Periodontics Restorative Dent*. 2014;34:e102–e111.

22. Schwarz F, Herten M, Sager M, Bieling K, Sculean A, Becker J. Comparison of naturally occurring and ligature-induced peri-implantitis bone defects in humans and dogs. *Clin Oral Implants Res*. 2007;18:161–170.

23. Cha JK, Paeng K, Jung UW, Choi SH, Sanz M, Sanz-Martin I. The effect of five mechanical instrumentation protocols on implant surface topography and roughness: a scanning electron microscope and confocal laser scanning microscope analysis. *Clin Oral Implants Res*. 2019;30:578–587.

24. de Tapia B, Valles C, Ribeiro-Amaral T, et al. The adjunctive effect of a titanium brush in implant surface decontamination at peri-implantitis surgical regenerative interventions: a randomized controlled clinical trial. *J Clin Periodontol*. 2019;46:586–596.

25. Sahrmann P, Gilli F, Wiedemeier DB, Attin T, Schmidlin PR, Karygianni L. The microbiome of peri-implantitis: a systematic review and meta-analysis. *Microorganisms*. 2020;8:661.

26. Liu Y, Qin R, Zaat SAJ, Breukink E, Heger M. Antibacterial photodynamic therapy: overview of a promising approach to fight antibiotic-resistant bacterial infections. *J Clin Transl Res*. 2015;1:140–167.

27. Solakoglu O, Filippi A. Regenerative therapy of peri-implantitis: clinical and radiologic documentation of 16 consecutive patients with a mean follow-up of 3 years. *J Oral Implantol*. 2019;45:145–153.

28. Lollobrigida M, Fortunato L, Serafini G, et al. The prevention of

implant surface alterations in the treatment of peri-implantitis: comparison of three different mechanical and physical treatments. *Int J Environ Res Public Health*. 2020;17:2624.

29. Park JB, Jeon Y, Ko Y. Effects of titanium brush on machined and sand-blasted/acid-etched titanium disc using confocal microscopy and contact profilometry. *Clin Oral Implants Res*. 2015;26:130–136.

30. Saffarpour A, Nozari A, Fekrazad R, Saffarpour A, Heibati MN, Iranparvar K. Microstructural evaluation of contaminated implant surface treated by laser, photodynamic therapy, and chlorhexidine 2 percent. *Int J Oral Maxillofac Implants*. 2018;33:1019–1026.

31. Sinjab K, Garaicoa-Pazmino C, Wang HL. Decision making for management of periimplant diseases. *Implant Dent*. 2018;27:276–281.

32. Urban IA, Monje A, Lozada J, Wang HL. Principles for vertical ridge augmentation in the atrophic posterior mandible: a technical review. *Int J Periodontics Restorative Dent*. 2017;37:639–645.